ISSN 1674-1056
http://cpb.iphy.ac.cn
http://iopscience.iop.org/cpb
中国物理 B
Chinese Physics
中国物理 Chinese Physics B

Superhard monoclinic BC_6N allotropes: First-principles investigations

Nian-Rui Qu(屈年瑞), Hong-Chao Wang(王洪超), Qing Li(李青), Yi-Ding Li(李一鼎), Zhi-Ping Li(李志平), Hui-Yang Gou(缑慧阳), Fa-Ming Gao(高发明)

Citation: Chin. Phys. B . 2019, 28(9): 096201 . **doi:** 10.1088/1674-1056/28/096201
Journal homepage: http://cpb.iphy.ac.cn; http://iopscience.iop.org/cpb

What follows is a list of articles you may be interested in

Orientation dependence of elastic properties in orthorhombic $Ca_3Mn_2O_7$

Gang Jian(简刚), Mei-Rui Liu(刘美瑞), Chen Zhang(张晨), Jie Lu(卢杰), Chao Yan(晏超)
Chin. Phys. B . 2019, 28(2): 026201 . **doi:** 10.1088/1674-1056/28/2/026201

First-principles investigations on structural stability, mechanical, and thermodynamic properties of LaT_2Al_{20} (T=Ti, V, Cr, Nb, and Ta) intermetallic cage compounds

Shanyu Quan(权善玉), Xudong Zhang(张旭东), Cong Liu(刘聪), Wei Jiang(姜伟)
Chin. Phys. B . 2018, 27(12): 126201 . **doi:** 10.1088/1674-1056/27/12/126201

Stability, elastic anisotropy, and electronic properties of Ca_2C_3

Quan Zhang(张权), Qun Wei(魏群), Hai-Yan Yan(闫海燕), Xuan-Min Zhu(朱轩民), Jun-Qin Zhang(张军琴), Xiao-Fei Jia(贾晓菲), Rong-Hui Yao(姚荣辉)
Chin. Phys. B . 2017, 26(6): 066201 . **doi:** 10.1088/1674-1056/26/6/066201

Elastic properties and electronic structures of lanthanide hexaborides

Duan Jie, Zhou Tong, Zhang Li, Du Ji-Guang, Jiang Gang, Wang Hong-Bin
Chin. Phys. B . 2015, 24(9): 096201 . **doi:** 10.1088/1674-1056/24/9/096201

Structural and mechanical stability of rare-earth diborides

Haci Ozisik, Engin Deligoz, Kemal Colakoglu, Gokhan Surucu
Chin. Phys. B . 2013, 22(4): 046202 . **doi:** 10.1088/1674-1056/22/4/046202

Surperhard monoclinic BC_6N allotropes: First-principles investigations*

Nian-Rui Qu(屈年瑞)[1], Hong-Chao Wang(王洪超)[1], Qing Li(李青)[1], Yi-Ding Li(李一鼎)[1], Zhi-Ping Li(李志平)[1,†], Hui-Yang Gou(缑慧阳)[2], and Fa-Ming Gao(高发明)[1,‡]

[1] *Key Laboratory of Applied Chemistry, Yanshan University, Qinhuangdao* 066004, *China*
[2] *Center for High Pressure Science and Technology Advanced Research, Beijing* 100094, *China*

(Received 17 June 2019; revised manuscript received 10 July 2019; published online 30 August 2019)

Via structural searching methodology and first-principles calculations, we predicted two new BC_6N allotropes, a C-centered monoclinic BC_6N (Cm-BC_6N) and a primitive-centered monoclinic BC_6N (Pm-BC_6N). The lattice vibrations, elastic properties, ideal strength, theoretical hardness, and electronic structure of the predicted BC_6N were investigated systematically. Our results reveal that Cm-BC_6N is more favorable energetically than graphite-like g-BC_6N above 20.6 GPa, which is lower than the transition pressures of r-BC_6N, t-BC_6N, and Pm-BC_6N. Both Cm-BC_6N and Pm-BC_6N are indirect semiconductors with band gaps of 2.66 eV and 0.36 eV, respectively. Cm-BC_6N exhibits the excellent ideal shear strength of 53.9 GPa in (011)[01$\bar{1}$], much greater than that of Pm-BC_6N (25.0 GPa in (010)[101] shear direction), and Cm-BC_6N shows a much lower anisotropy in shear strength than Pm-BC_6N. The Vickers hardness of Cm-BC_6N is estimated to be above 80 GPa, which is more outstanding than those of t-BC_6N and r-BC_6N.

Keywords: superhard materials, elastic properties, boron-carbon-nitride, ideal strength.

PACS: 62.20.–x **DOI:** 10.1088/1674-1056/ab3439

1. Introduction

Due to its broad industrial applications, superhard material is always of great scientific interest.[1,2] As we all know, the diamond and cubic boron nitride (c-BN) are well-studied superhard materials with excellent physical properties, such as wide band gaps, high hardness and thermal conductivity, large shear and bulk modules. However, the adhibition of diamond has been conditioned by its own imperfections, including brittleness, reacting with iron easily, and generating oxidizing reaction in the air at a high temperature. Cubic boron nitride shows better performance than diamond above, but its hardness and mechanical properties are obviously weaker than those of diamond.[3] B–C–N ternary system is considered to be harder and stronger than c-BN, chemically and thermally more stable than diamond.[4] Therefore, searching superhard materials from the B–C–N ternary system has been a focus of scientific research. Zhao *et al.*[5] successfully synthesized stoichiometric c-BC_2N and c-BC_4N crystals with diamond-like structures by using a diamond-anvil cell. Then Fan *et al.*[6–15] did systematic investigations of these structures based on the first-principles calculations, such as crystal structure, band gap, optical spectrum, ideal strength and hardness, in order to establish facts and reach new conclusions.

As we know that B–C–N compounds can consist of the typical sp^3 covalent bonds containing B–C, B–N, C–N, and C–C bonds, the mechanical properties thus would be better with the increase of carbon content.[16–18] Graphite-like BC_6N (g-BC_6N)[19] has been found as an n-type semiconductor, which was synthesized by the chemical vapor deposition. The diamond-like t-BC_6N and r-BC_6N were proposed by Luo *et al.*,[20] which were obtained by replacing two carbon atoms in the eight-atom cubic diamond unit cell with a nitrogen atom and a boron atom. According to their results, the Vickers hardness of the two BC_6N phases is about 80 GPa, higher than that of c-BN (66 GPa) and c-BC_2N (76 GPa). In fact, the first-principles and their evolution methods are always used in predicting possible crystal structures or interpreting the mechanical properties of superhard materials.[21,22]

In the present work, a C-centered monoclinic BC_6N (Cm-BC_6N) and a primitive-centered monoclinic BC_6N (Pm-BC_6N) are proposed by structure searching method based on first-principles calculations. The structural, electronic, and mechanical properties of the proposed BC_6N allotropes are investigated systematically. The Cm-BC_6N and Pm-BC_6N have dynamical and mechanical stability in ambient circumstance. We not only find their semiconductor nature from the band structures, but also can draw a conclusion that Cm-BC_6N is more favorable than the previous predicted t-BC_6N and r-BC_6N in thermodynamics. By computing the ideal strength and theoretical hardness, we find out the superhard nature structures.

*Project supported by the National Natural Science Foundation of China (Grant Nos. 21671168 and 21875205), the Hebei Natural Science Foundation, China (Grant No. B2015203096), and the Qinhuangdao Science and Technology Support Program, China (Grant No. 201703A014).

†Corresponding author. E-mail: zpli@ysu.edu.cn
‡Corresponding author. E-mail: fmgao@ysu.edu.cn

© 2019 Chinese Physical Society and IOP Publishing Ltd

2. Calculation method

Crystal structures of Cm-BC_6N and Pm-BC_6N were explored by using the evolutionary methodology through particle swarm optimization as implemented in CALYPSO package,[23,24] which has successfully predicted various structures.[25–28] Subsequent structural relaxation and property calculations were performed based on the density functional theory[29,30] with the Vienna *ab initio* simulation software package (VASP) code, with a projector augmented wave (PAW) scheme[31] to show the electrons–ion interaction. The generalized gradient approximation (GGA) with the Perdew–Burke–Ernzerhof (PBE)[32] functional was employed to describe the exchange and correlation potentials. From our text data, a plane-wave kinetic energy cutoff of 500 eV and quantitative value of *k*-points sampling of 0.25 $Å^{-1}$ in Brillouin zone were used to give good convergence of the total energies. Optimization of the internal atomic positions and the lattice parameters was achieved by the minimization of forces and stress tensors. After calculating the elastic constants, the bulk modulus and shear modulus were figured out following the Voigt–Reuss–Hill (VRH) approximations.[33] From the local density approximation in plane wave basis, the phonon dispersions were calculated by the density functional perturbation theory, which has been implemented the Quantum ESPRESSO code[34] with the Troullier–Martins (TM) pseudopotentials.[35] Static enthalpy differences calculated relative to the graphite-like g-BC_6N structure for the various structures are plotted in Fig. 2 as a function of pressure. The calculations of stress–strain relations were performed following the method of Refs. [36]–[38], which have calculated the strength of several strong solids successfully.[39,40] By the micro hardness models for covalent crystal, we acquired the hardness.[41–43]

3. Results and discussion

The optimized structures of Cm-BC_6N and Pm-BC_6N are shown in Figs. 1(a) and 1(b). Both of Cm-BC_6N and Pm-BC_6N have irregular six membered rings along the [100] and [010] directions. There are B–N bonds in Cm-BC_6N structure, which is the key distinction to Pm-BC_6N. All atoms are four coordinated with sp^3 hybridization, resulting in six membered rings like chair/boat. More detailed structure information of Cm-BC_6N and Pm-BC_6N is listed in Table 1. For comparison, the structure parameters of t-BC_6N and r-BC_6N are also provided. The unit cell of Cm-BC_6N contains sixteen atoms. Two B, two N, and four C atoms locate at four inequivalent crystallographic 2*a* sites, respectively. The other eight C atoms averagely locate at two inequivalent crystallographic 4*b* sites. The unit cell of Pm-BC_6N contains eight atoms. One B and three C (from C1 to C3) atoms locate at four inequivalent crystallographic 1*a* sites, respectively. One N and the other three C (from C4 to C6) atoms locate at four inequivalent crystallographic 1*b* sites, respectively. As shown in Table 1, the mass density of Cm-BC_6N (3.446 g/cm^3) is the largest among the BC_6N allotropes, suggesting that the spatial structure of Cm-BC_6N is the most compact one among them.

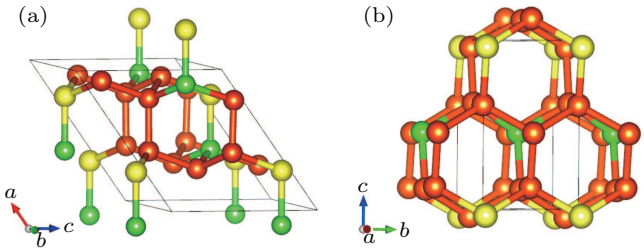


Fig. 1. Structures of (a) Cm-BC_6N and (b) Pm-BC_6N; the yellow, orange, and green spheres represent B, C, and N atoms, respectively.

Table 1. The equilibrium lattice parameters of *a*, *b*, *c*, density ρ, volume, and atomic positions.

structure	Cm-BC_6N	Pm-BC_6N	t-BC_6N		r-BC_6N
Symmetry	Cm (No. 8)	Pm (No. 6)	$P\bar{4}2m$ (No. 111)		$R3m$ (No. 160)
a/Å	5.088	4.232	3.611	3.574[a]	5.101
b/Å	5.102	2.54	3.611	3.574[a]	5.101
c/Å	4.407	4.406	3.603	3.564[a]	6.221
α/(°)	90	90	90		90
β/(°)	125.3	90.15	90		90
γ/(°)	90	90	90		120
ρ/g·cm^{-3}	3.446	3.396	3.424	3.535[a]	3.443
Volume/Å^3	93.365	47.37	46.988	45.512[a]	140.188
Atomic positions	B(0.281, 0, 0.94)	B(0.102, 0, 0.959)	/		/
	C1(0.282, 0.5, 0.94)	C1(0.978, 0, 0.616)			
	C2(0.412, 0, 0.686)	C2(0.484, 0, 0.957)			
	C3(0.781, 0.251, 0.435)	C3(0.609, 0, 0.626)			
	C4(0.908, 0.243, 0.192)	C4(0.978, 0.5, 0.128)			
	N(0.399, 0.5, 0.686)	C5(0.615, 0.5, 0.116)			
		C6(0.089, 0.5, 0.449)			
		N(0.473, 0.5 ,0.453)			

[a]Ref. [20].

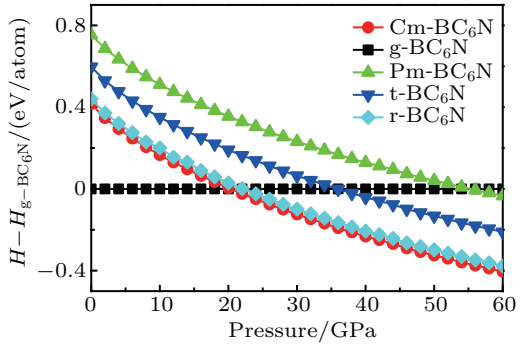


Fig. 2. Enthalpy as a function of pressure for BC_6N allotropes relative to g-BC_6N.

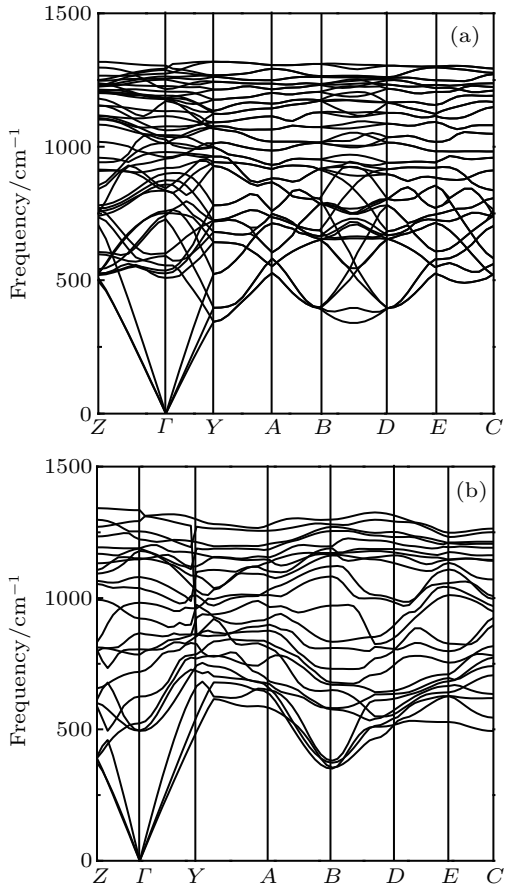


Fig. 3. The phonon-dispersion curves of (a) Cm-BC_6N and (b)Pm-BC_6N at 0 GPa.

To assess the thermodynamic stability of the BC_6N (Cm-BC_6N, Pm-BC_6N, t-BC_6N, and r-BC_6N) phases, the relative enthalpies (without temperature effect) are calculated at the pressure range of 0–60 GPa. The pressure–enthalpy relationship calculated for all BC_6N phases is shown in Fig. 2. At zero pressure, g-BC_6N is the most stable phase, and Cm-BC_6N, Pm-BC_6N, t-BC_6N, and r-BC_6N are higher than g-BC_4N by 0.42 eV, 0.75 eV, 0.60 eV, and 0.44 eV per atom, respectively. The enthalpy of Cm-BC_6N is the lowest among the other phases within the entire pressure range, suggesting that Cm-BC_6N should be accessed more easily than Pm-BC_6N, t-BC_6N, and r-BC_6N. Under hydrostatic compression, Cm-BC_6N becomes more favorable energetically than g-BC_6N above 20.6 GPa; and it has a lower transition pressure than 22.2 GPa for r-BC_6N, 35.8 GPa for t-BC_6N, and 55.5 GPa for Pm-BC_6N. Moreover we calculate the phonon dispersion to prove the dynamical stability of Cm-BC_6N and Pm-BC_6N. As shown in Fig. 3, there are no imaginary frequencies observed in the whole Brillouin zone, which indicates that the two phases keep dynamically stable at zero pressure.

By the Hooke's law, we calculate the single-crystal zero-pressure elastic constants C_{ij} to comprehend Cm-BC_6N and Pm-BC_6N in elastic stability and mechanical properties.[44] For monoclinic symmetry, there are thirteen independent single-crystal elastic constants. As shown in Table 2, the calculated elastic stiffness constants C_{ij} of Cm-BC_6N and Pm-BC_6N satisfy the mechanical stability criteria for a monoclinic structure,[45] indicating the elastically stability at ambient condition.

Table 2. Calculated zero-pressure elastic constants C_{ij} (GPa), bulk modulus B (GPa), shear modulus G (GPa), Young's modulus E (GPa), and Poisson's ratio υ of Cm-BC_6N and Pm-BC_6N.

Phase	Cm-BC_6N	Pm-BC_6N	t-BC_6N	r-BC_6N
C_{11}	1085.3	1034.8	935.8	1007.2
C_{22}	1026.3	983.7		
C_{33}	1014.9	979.4	913.8	1095.4
C_{44}	474.8	442.1	481.9	439.8
C_{55}	441.8	384.1		
C_{66}	436.4	368.4	488.0	457.7
C_{12}	59.0	40.6	123.3	91.8
C_{13}	62.0	26.5	105.5	61.9
C_{14}				39.2
C_{15}	–3.0	–0.5		
C_{23}	94.9	115.9		
C_{25}	46.0	–20.5		
C_{35}	–40.4	34.8		
C_{46}	41.8	–30.8		
B_V	395.3	373.8	383.8	393.4
B_R	395.3	373.6	383.6	393.2
G_V	464.6	426.6	453.8	460.4
G_R	459.9	419.4	450.6	456.2
B	395.3	373.7	383.7	393.3
G	462.3	423.0	452.2	458.3
E	997.8	921.3	974.0	990.3
B/G	0.86	0.88	0.85	0.86
υ	0.08	0.09	0.08	0.08

Superhard materials not only manifest high bulk and shear moduli but also exhibit low Poisson's ratio, because of hardness strongly depending on the plastic deformation.[41] Additionally, the Voigt–Reuss–Hill approximation is used to reckon the polycrystalline elastic moduli as the C_{ij} have been calculated, and the results are listed in Table 2. The calculated bulk modulus of Cm-BC_6N (395.3 GPa) within GGA in the present work is the greatest one, followed by r-BC_6N (393.3 GPa), t-BC_6N (383.7 GPa), and Pm-BC_6N (373.7 GPa). Note that the bulk moduli of t-BC_6N and r-BC_6N are 410.4 GPa and 399.9 GPa in Ref. [20]. The order of shear modulus is the same as that of bulk modulus: Cm-BC_6N

(462.3 GPa) > r-BC_6N (458.3 GPa) > t-BC_6N (452.2 GPa) > Pm-BC_6N (423.0 GPa). When describing the directional degree of covalent bonds about a material, we always choose another momentous parameter called Poisson's ratio υ. All of the proposed phases have low Poisson's ratio (0.08–0.09), which indicates the possibilities of directional covalent bonding. Furthermore, all the BC_6N phases exhibit the brittle behavior due to the low ratio of B/G (0.85–0.88) according to Pugh's rule.[46]

The Young's module (E) is one of the most important parameters which measures the stiffness of a solid material. We show the three-dimensional (3D) representation and the corresponding two-dimensional (2D) projection of the Young's modulus for Cm-BC_6N and Pm-BC_6N and in Fig. 4. The shape of the 3D curved surface of Cm-BC_6N is close to a sphere and the 2D projections in the xz, yz, and xy planes are close to a circle, which show that Cm-BC_6N has slight anisotropy. The same thing happens to Pm-BC_6N. As can be seen in Fig. 4, the xz, yz, and xy plane areas of Cm-BC_6N are larger than those of Pm-BC_6N, indicating that the Young's modulus property of Cm-BC_6N is superior to that of Pm-BC_6N.[47]

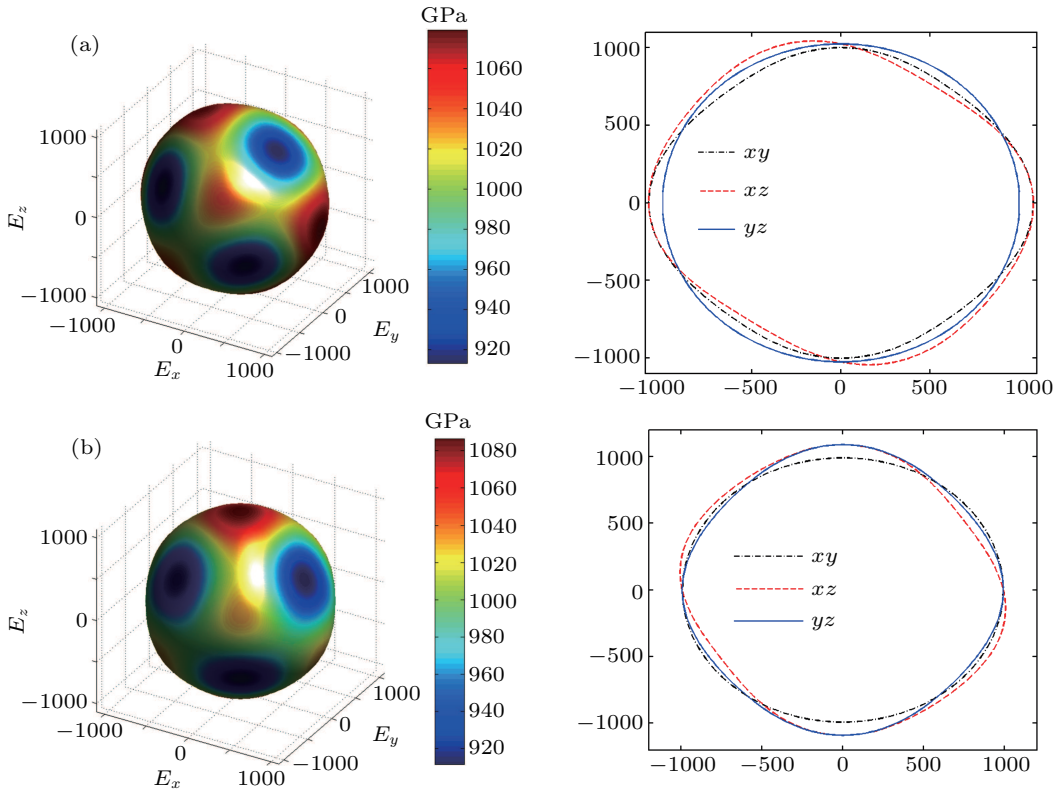


Fig. 4. The 3D representations (left panel) and 2D projections (right panel) of Young's moduli for (a) Cm-BC_6N and (b) Pm-BC_6N. Note that the negative sign only denotes the direction corresponding to the positive one.

The calculated electronic band structure and density of states (DOS) of Cm-BC_6N and Pm-BC_6N at 0 GPa are presented in Fig. 5. It can be seen from the left panel of Fig. 5 that Cm-BC_6N and Pm-BC_6N are semiconductor with an indirect band gap of 2.66 eV and 0.36 eV, respectively. The band gap of Cm-BC_6N is larger than that of the previous proposed r-BC_6N (2.09 eV) and t-BC_6N (2.06 eV). The band gap of Pm-BC_6N (0.36 eV) is the smallest among them. From the data, Cm-BC_6N has the top of the valence band at Γ point and the bottom of the conduct band at Z point. Pm-BC_6N has the top of the valence band at Γ point and the bottom of the conduct band at E point.

To further understand the chemical bonding and electronic properties, we calculate the partial density of states (PDOS) of Cm-BC_6N and demonstrate the primary valence-electron states of B, C, and N atoms. From the right panel of Fig. 5, it can be find out that there are harmonic 2p–2s overlaps between B(C, N)-2s and B(C, N)-2p states over the whole valence bands in both Cm-BC_6N and Pm-BC_6N structures, which ascertains the hybridization of the s and p orbitals and the strong interaction between B, C, and N atoms. It is in accordance with the bonding behaviors in the previous reports of B–C–N system. In Cm-BC_6N, the B(C, N)-2s mainly contributes to the valence bands below about 10.0 eV, and the B(C, N)-2p mainly contributes to the valence bands between about 10.0 eV and 0 eV. We note the nonmetallic nature of Cm-BC_6N by the large energy band gap which is clear and near the Fermi level.

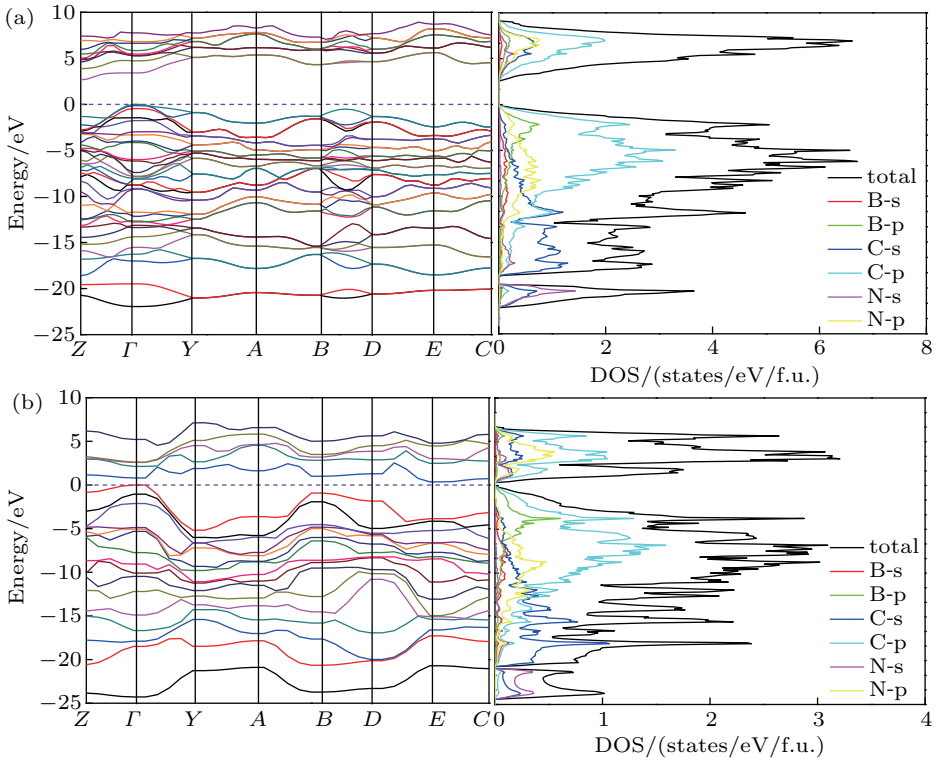


Fig. 5. Electronic band structures (left panel) and density of states (right panel) of (a) Cm-BC_6N and (b) Pm-BC_6N. The energy is measured from the valence top.

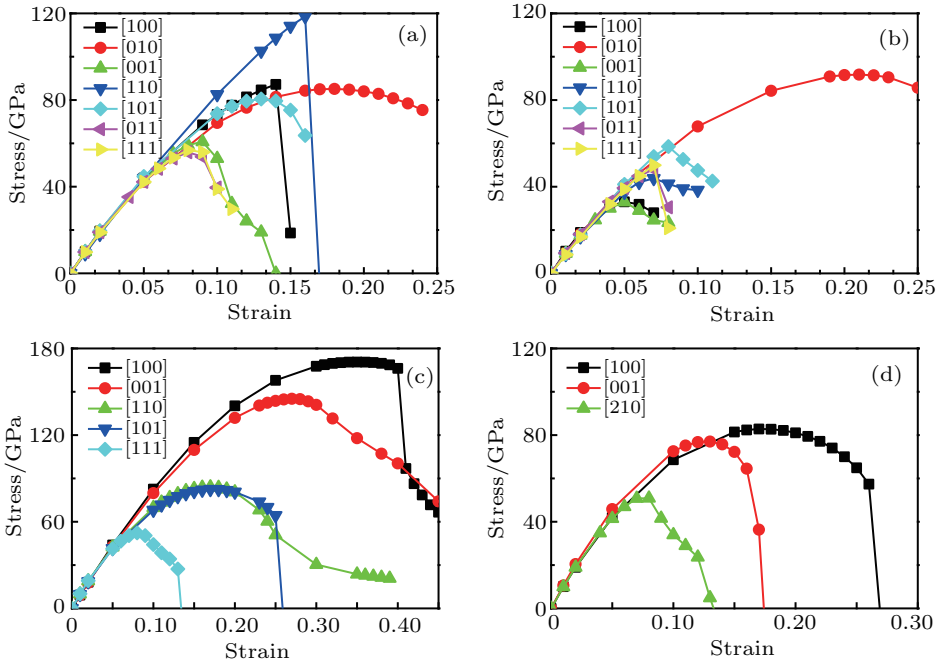


Fig. 6. Calculated tensile stress versus tensile strain for (a) Cm-BC_6N, (b) Pm-BC_6N, (c) t-BC_6N, and (d) r-BC_6N in principal symmetry directions.

We also calculate the ideal strength to connect the atomic level strength under plastic deformation and permanent large strain.[48,49] The calculated tensile stress versus tensile strain of Cm-BC_6N, Pm-BC_6N, t-BC_6N, and r-BC_6N are shown in Fig. 6. As shown in Fig. 6(a), the stress responses of Cm-BC_6N in the seven principal directions with the peak tensile stresses are within the range of 55.9–118.6 GPa. The anisotropy ratio of the ideal tensile strengths for Cm-BC_6N is $\sigma[110] : \sigma[100] : \sigma[010] : \sigma[101] : \sigma[001] : \sigma[111] : \sigma[011] \approx$ 118.6 GPa : 87.2 GPa : 85.1 GPa : 80.5 GPa : 60.7 GPa: 56.9 GPa : 55.9 GPa $\approx 2.12 : 1.56 : 1.52 : 1.44 : 1.09 : 1.02 : 1$. Nevertheless, the weakest tensile strength of Cm-BC_6N is 55.9 GPa in the [011] direction at a strain of 0.08. As shown in Fig. 6(b), the strong stress responses in the seven principal directions with the peak tensile stresses are between 32.9 GPa and 91.8 GPa for Pm-BC_6N. The

anisotropy ratio of the ideal tensile strengths for Pm-BC_6N is $\sigma[010]:\sigma[101]:\sigma[111]:\sigma[011]:\sigma[110]:\sigma[100]:\sigma[001] \approx 91.8$ GPa : 58.5 GPa : 49.9 GPa : 48.1 GPa : 43.9 GPa : 33.0 GPa : 32.9 GPa $\approx 2.79:1.78:1.52:1.46:1.33:1.00:1$. Nevertheless, the weakest tensile strength of Pm-BC_6N is 32.9 GPa in the [001] direction at a strain of 0.05. As shown in Fig. 6(c), the strong stress responses in the five principal directions with the peak tensile stresses are between 52.3 GPa and 170.6 GPa for t-BC_6N. The anisotropy ratio of the ideal tensile strengths for t-BC_6N is $\sigma[100]:\sigma[001]:\sigma[110]:\sigma[101]:\sigma[111] \approx 170.6$ GPa : 145.1 GPa : 84.1 GPa : 82.4 GPa : 52.3 GPa $\approx 3.26:2.78:1.61:1.58:1$. Nevertheless, the weakest tensile strength of t-BC_6N is 52.3 GPa in the [111] direction at a strain of 0.08. From Fig. 6(d), we find that with the peak tensile stresses, the strong stress responses in the three prime directions are within 82.8–50.9 GPa for r-BC_6N. The anisotropy ratio of the ideal tensile strengths for r-BC_6N is $\sigma[100]:\sigma[001]:\sigma[210] \approx 82.8$ GPa : 77.0 GPa : 50.9 GPa $\approx 1.63:1.51:1$. Nevertheless, the weakest tensile strength of r-BC_6N is 50.9 GPa in the [210] direction at a strain of 0.08. From the data above, the weakest tensile strength of Cm-BC_6N is the largest among the BC_6N allotropes, whereas the weakest tensile strength of Pm-BC_6N is the smallest. Both of the ideal tensile strengths of Cm-BC_6N and Pm-BC_6N are significantly larger than that of β-BC_2N.[50]

We also investigate the stress–strain relations of Cm-BC_6N and Pm-BC_6N in various principal symmetry directions under shear deformation. The anisotropy ratio of the ideal shear strengths for Cm-BC_6N is $\sigma(100)[001]:\sigma(011)[100]:\sigma(110)[1\bar{1}0]:\sigma(100)[010]:\sigma(110)[1\bar{1}1]:\sigma(100)[011]:\sigma(011)[11\bar{1}]:\sigma(110)[001]:\sigma(011)[01\bar{1}] \approx 107.4:83.8:78.0:77.7:76.7:66.5:65.3:57.6:53.9 = 1.99:1.55:1.45:1.44:1.42:1.23:1.21:1.07:1$. The weakest shear strength of 53.9 GPa of Cm-BC_6N is found along the $(011)[01\bar{1}]$ shear deformation path. The anisotropy ratio of the ideal shear strengths for Pm-BC_6N is $\sigma(001)[100]:\sigma(001)[110]:\sigma(010)[100]:\sigma(101)[11\bar{1}]:\sigma(101)[010]:\sigma(010)[001]:\sigma(001)[010]:\sigma(101)[10\bar{1}]:\sigma(010)[101] \approx 87.9:46.9:34.2:31.4:30.5:29.6:27.7:26.7:25.0 = 3.52:1.88:1.37:1.26:1.22:1.19:1.11:1.07:1$. The weakest shear strength of 25.0 GPa of Pm-BC_6N is found along the (010)[101] shear deformation path. The magnitude of the ideal shear strength of Cm-BC_6N approaches to 58.3 GPa found for the $(111)[11\bar{2}]$ slip system of c-BN.[51] Besides, it is found that the lowest peak shear stresses of Cm-BC_6N and Pm-BC_6N are lower than their lowest peak tensile stress, respectively, indicating that the mechanical failure modes of these two BC_6N allotropes are dominated by the shear type.

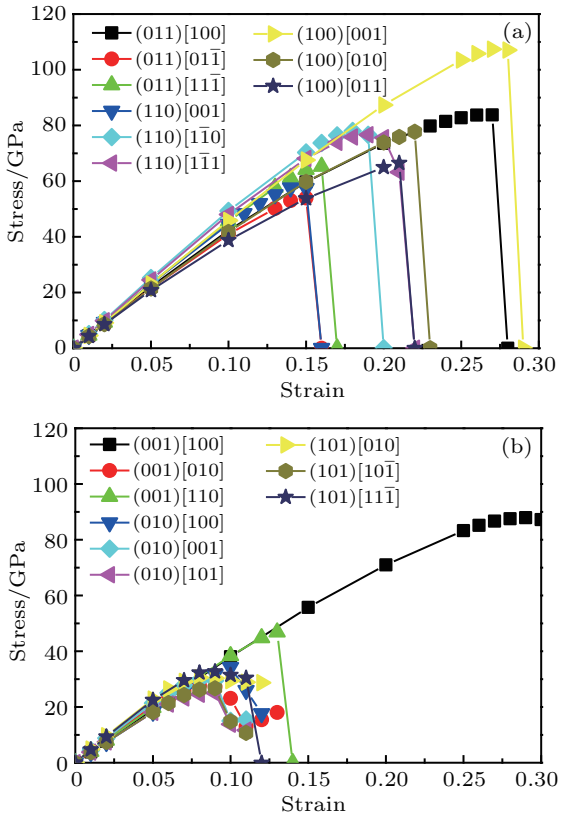


Fig. 7. Calculated shear stress versus shear strain for (a) Cm-BC_6N and (b) Pm-BC_6N in principal symmetry directions.

Due to the connection of the hardness and the bulk modulus or shear modulus, we can acquire the hardness. The hardness calculations are performed based on the microscopic models of hardness constructed by Gao *et al.*[41–43] and Chen *et al.*[52,53] respectively, which have been widely applied currently. In Gao's microscopic hardness models, the hardness of a covalent material is determined by two factors: the properties of bonding at equilibrium and the number of bonds per unit area. The later includes the bond length, charge density, iconicity, etc. The Vickers hardness H_v^μ of the μ-type bond can be calculated as follows:

$$H_v^\mu(\mathrm{GPa}) = 8.82(N_e^\mu)^{2/3}E_h^\mu\, e^{-1.191 f_i^\mu}, \quad (1)$$

where N_e^μ is the number of valence electrons of the μ-type bonds per cubic angstroms, and it is determined by the number of effective valence electrons per μ bond $(n_e^\mu)^*$ and the bond volume v_b^μ, which can be expressed as $N_e^\mu = (n_e^\mu)^*/v_b^\mu$. E_h^μ is Phillips's homopolar band gap of the μ-type bonds,[54] which characterizes the strength of the covalent bond.[41] f_i is ionicity of chemical bond in crystal scaled by Phillips,[55] and $f_i^\mu = 1-(E_h^\mu)^2/(E_g^\mu)^2$, where $E_h^\mu = 39.74/(d^\mu)^{2.5}$ and $(E_g^\mu)^2 = (E_h^\mu)^2 + (C^\mu)^2$.

In practical applications, we define the geometric average hardness of all kinds of chemical bonds in crystals as follows:

$$H_{\mathrm{Vav.}} = \left[\prod^{\mu}(H_v^\mu)^{n^\mu}\right]^{1/\sum n^\mu}, \quad (2)$$

where n^{μ} is the number of the μ-type bonds composing the actual complex crystal.

We calculate the atomic bond hardness of BC_6N and show the result in Table 3, and the calculation results of c-BC_4N, β-BC_2N, c-BN, and diamond are also given for comparison. The theoretical Vickers hardness values of r-BC_6N (80.2 GPa) and t-BC_6N (80.0 GPa) are according with the calculation results of Ref. [20]. The theoretical Vickers hardness values of c-BC_4N(80.3 GPa) and β-BC_2N(75.5 GPa) agree well with experimental results of Refs. [15] and [6]. This proves the reliability. The hardness values of Cm-BC_6N and Pm-BC_6N are predicted to be 80.6 GPa and 77.4 GPa by Gao's model and to be 84.0 GPa and 76.5 GPa by Chen's model, respectively. Coincidently, the hardness H_v by Chen's model is compared favorably with $H_{Vav.}$ for the two novel BC_6N allotropes. Both methods indicate that Cm-BC_6N is a superhard material with the high Vickers hardness above 80 GPa, which is evidently larger than that of c-BN (66.4 GPa), β-BC_2N (75.5 GPa), and c-BC_4N (80.3 GPa); furthermore, Cm-BC_6N is harder than r-BC_6N (80.2 GPa) and t-BC_6N (80.0 GPa); nevertheless, it is slightly inferior to diamond (93.8 GPa). The results show the superior mechanical properties of Cm-BC_6N and Pm-BC_6N in potential technological applications.

Table 3. Hardness calculations of Cm-BC_6N, Pm-BC_6N, t-BC_6N, r-BC_6N, c-BC_4N, c-BN, and diamond, where d^{μ} is the bond length, N_e^{μ} is the electron density expressed in number of valence electrons per cubic angstroms, E_h^{μ} is the homopolar gap, E_g^{μ} is the valence-conduction band gap, f_i^{μ} is the ionicity of bond, $H_{Vav.}$ is geometric average of all bonds vickers hardness, compared to the hardness of H_v (Chen) and the experimental hardness $H_{exp.}$, respectively.

Phase	Bond	N_e^{μ}	d^{μ}/Å	Population	v_b^{μ}/Å^3	N_e^{μ}/Å^{-3}	E_h^{μ}/eV	E_g^{μ}/eV	f_i^{μ}	H_v^{μ}/GPa	$H_{Vav.}$/GPa	$H_{vcal.}$/GPa	H_v(Chen)/GPa	$H_{exp.}$/GPa
Cm–BC_6N	B–C_3	2	1.599	0.77	3.145	0.445	12.286	12.294	0.001	63.1	80.6		84.0	
	B–C_1	4	1.592	0.92	3.104	0.533	12.423	12.448	0.004	71.7				
	B–N	2	1.589	0.62	3.085	0.569	12.486	15.190	0.324	51.4				
	C_1–C_2	4	1.548	0.81	2.851	0.739	13.333	13.373	0.006	95.5				
	C_3–C_4	2	1.533	0.82	2.773	0.777	13.648	13.664	0.002	101.5				
	C_1–C_2	4	1.542	0.83	2.817	0.766	13.466	13.508	0.006	98.7				
	C_1–C_4	4	1.538	0.89	2.795	0.827	13.557	13.599	0.006	104.6				
	C_2–C_3	4	1.559	0.89	2.916	0.803	13.086	13.106	0.003	99.4				
	C_4–N	2	1.542	0.63	2.820	0.632	13.457	16.346	0.322	59.6				
	C_2–N	4	1.565	0.69	2.947	0.663	12.972	16.107	0.351	57.3				
Pm-BC_6N	B–C_1	1	1.616	0.43	3.241	0.267	11.970	11.974	0.001	43.8	77.4		76.5	
	B–C_4	1	1.599	0.65	3.136	0.413	12.301	12.317	0.003	60.0				
	B–C_6	2	1.566	0.92	2.946	0.614	12.959	13.016	0.009	81.7				
	C_5–C_6	1	1.534	0.62	2.772	0.724	13.634	13.671	0.005	96.3				
	C_3–C_4	1	1.563	0.66	2.933	0.759	13.007	13.086	0.012	94.1				
	C_2–C_6	1	1.490	0.74	2.542	0.943	14.654	14.707	0.007	123.2				
	C_1–C_3	1	1.550	0.81	2.861	0.966	13.280	13.341	0.009	113.2				
	C_2–C_4	2	1.540	0.90	2.805	0.843	13.500	13.518	0.003	105.9				
	C_1–C_5	2	1.554	0.90	2.880	0.829	13.208	13.211	0.000	102.8				
	C_2–N	1	1.626	0.44	3.303	0.415	11.781	13.807	0.272	41.8				
	C_5–N	1	1.601	0.57	3.153	0.563	12.246	15.122	0.344	48.9				
	C_3–N	2	1.590	0.68	3.084	0.699	12.473	15.708	0.369	55.8				
t-BC_6N	C_1–N	4	1.571	0.60	2.986	0.631	12.838	15.583	0.321	56.8	80.0	79.9[a]	83.7	
	B–C_1	4	1.574	0.72	3.000	0.504	12.791	12.792	0.000	71.4				
	C_1–C_2	8	1.553	0.76	2.880	0.809	13.230	13.274	0.007	100.5				
c-BC_6N	B–N	3	1.576	0.64	3.013	0.335	12.740	13.004	0.040	51.7	80.2	79.1[a]	83.2	
	C_1–C_2	9	1.539	0.85	2.804	0.899	13.526	13.567	0.006	110.3				
	C_1–N	9	1.572	0.68	2.991	0.633	12.818	15.787	0.341	55.5				
	B–C_2	9	1.578	0.89	3.025	0.520	12.699	12.713	0.002	72.3				
	C_1–C_2	18	1.552	0.87	2.876	0.718	13.246	13.277	0.005	93.1				
c-BC_4N	B–C_3	1	1.617	0.51	3.235	0.342	11.946	12.0-24	0.013	50.7	80.3	84.3[b]	81.4	85±4[c]
	B–N	3	1.566	0.69	2.938	0.735	12.944	15.031	0.258	68.3				
	C_4–C_3	3	1.550	0.83	2.850	0.843	13.278	13.278	0.000	104.5				
	C_4–C_1	1	1.554	0.50	2.872	0.349	13.193	13.193	0.000	57.7				
	C_2–C_1	3	1.549	0.83	2.850	0.849	13.306	13.307	0.000	105.2				
	C_2–N	1	1.516	0.47	2.842	0.494	14.052	16.080	0.236	58.4				
β-BC_2N	C_1–C_2	4	1.528	0.83	2.744	0.911	13.767	13.767	0	114.1	75.5		75.4	76[d]
	B–C_1	4	1.591	0.72	3.094	0.485	12.453	12.453	0	67.8				
	C_2–N	4	1.578	0.59	3.021	0.662	12.706	14.49	0.231	64.6				
	B–N	4	1.576	0.62	3.011	0.664	12.741	14.528	0.231	65.0				
Diamond	C–C	16	1.544	0.75	2.834	0.706	13.413	13.413	0	93.8	93.8		93.6	96±5[e]
c-BN	B–N	16	1.569	0.65	2.973	0.673	12.889	14.691	0.23	66.4	66.4		63.5	63±5[e]

[a]Ref. [20], [b]Ref. [7], [c]Ref. [15], [d]Ref. [6], [e]Ref. [41].

4. Conclusion

In summary, two superhard BC_6N with monoclinic structures were proposed. The structural, electronic, and mechanical properties were investigated by first-principles calculations. Cm-BC_6N and Pm-BC_6N are both mechanically and dynamically stable, and Cm-BC_6N is suggested to be more easily synthesized than Pm-BC_6N, t-BC_6N, and r-BC_6N. We found that the lowest stress peak of Cm-BC_6N is 53.9 GPa, which is higher than that of other general hard materials. Comparing with other BCN allotropes which have been proposed and Pm-BC_6N, Cm-BC_6N has a higher hardness from Gao's model (80.6 GPa). In Cm-BC_6N, the B and N atoms connect each other by the prominent and strong C–C bond which results in its superior mechanical properties. Both of Cm-BC_6N and Pm-BC_6N are significantly harder than β-BC_2N and c-BN, suggesting the intrinsic superhard materials.

References

[1] Haines J, Leger J and Bocquillon G 2001 *Annu. Rev. Mater. Res.* **31** 1
[2] Liu A Y and Cohen M L 1989 *Science* **245** 841
[3] Wentorf R H Jr. 1957 *J. Chem. Phys.* **26** 956
[4] Horridge G A, Kuck S, Petermann K, Pohlmann U, Huber G, Nozaki H and Itoh S 1996 *J. Phys. Chem. Solids* **57** 41
[5] Zhao Y, He D W, Daemen L L, Shen T D, Schwarz R B, Zhu Y, Bish D L, Huang J, Zhang J, Shen G, Qian J and Zerda T W 2002 *J. Mater. Res.* **17** 3139
[6] Fan X F, Wu H Y, Shen Z X and Kuo J L 2009 *Diamond & Relat. Mater.* **18** 1278
[7] Luo X G, Zhou X F, Liu Z Y, He J L, Xu B, Yu D L, Wang H T and Tian Y J 2008 *J. Phys. Chem. C* **112** 9516
[8] Luo X G, Guo X J, Xu B, Wu Q, Hu Q, Liu Z, He J, Yu D, Tian Y and Wang H T 2007 *Phys. Rev. B Condens. Matter* **76** 094103
[9] Chen S Y, Gong X G and Wei S 2007 *Phys. Rev. Lett.* **98** 015502
[10] Qu N R, Wang H C, Li Q, Li Z P and Gao F M 2019 *Chin. Phys. Lett.* **36** 036201
[11] Hou L, Gao F M, Gou H Y, Wang Z B and Tian M 2008 *Cryst. Growth & Des.* **8** 1972
[12] Zang C P and Sun H 2010 *Phys. Rev. B* **81** 012106
[13] Chen Z Q, Li C M, Wang J, Wang F and Wang Q 2013 *Sci. Sin.* **43** 142
[14] Wang D, Shi R and Gan L H 2017 *Chem. Phys. Lett.* **669** 80
[15] Tang M J, He D W, Wang W D, Wang H K, Xu C, Li F J and Guan J W 2012 *Scr. Mater.* **66** 781
[16] Zhang Y, Sun H and Chen C F 2008 *Phys. Rev. B* **77** 094120
[17] Li F, Man Y H, Li C M, Wang J P and Chen Z Q 2015 *Comput. Mater. Sci.* **102** 327
[18] Chen S Y, Gong X G and Wei S H 2008 *Phys. Rev. B* **77** 014113
[19] Kawaguchi, Wakukawa and Kawano 2001 *Synth. Met.* **125** 259
[20] Luo X G, Guo X J, Liu Z Y, He J L, Yu D L, Tian Y J and Wang H T 2007 *J. Appl. Phys.* **101** 083505
[21] Zhang X X, Wang Y C, Lv J, Zhu C Y, Li Q, Zhang M, Li Q and Ma Y M 2013 *J. Chem. Phys.* **138** 114101
[22] Ullah S, Wang L, Li J X, Li R H and Chen X Q 2019 *Chin. Phys. B* **28** 077105
[23] Wang Y C, Lv J, Zhu L and Ma Y M 2010 *Phys. Rev. B* **82** 094116
[24] Wang Y, Lv J, Zhu L and Ma Y 2012 *Comput. Phys. Commun.* **183** 2063
[25] Li Q, Ma Y M, Oganov A R, Wang H B, Wang H, Xu Y, Cui T, Mao H K and Zou G T 2009 *Phys. Rev. Lett.* **102** 175506
[26] Lv J, Wang Y C, Zhu L and Ma Y M 2011 *Phys. Rev. Lett.* **106** 015503
[27] Li Q, Zhou D, Zheng W T, Ma Y M and Chen C F 2013 *Phys. Rev. Lett.* **110** 136403
[28] Li Y, Hao J, Liu H Y, Lu S Y and Tse J S 2015 *Phys. Rev. Lett.* **115** 105502
[29] Hohenberg P and Kohn W 1964 *Phys. Rev.* **136** B864
[30] Kohn W and Sham L J 1965 *Phys. Rev.* **140** A1133
[31] Blöchl P E 1994 *Phys. Rev. B* **50** 17953
[32] Perdew J P, Burke K and Ernzerhof M 1996 *Phys. Rev. Lett.* **77** 3865
[33] Ding Y 2012 *Physica B* **407** 2282
[34] Lazzeri M and Mauri F 2003 *Phys. Rev. Lett.* **90** 036401
[35] N Troullier J L M 1991 *Phys. Rev. B* **43** 1993
[36] Roundy D, Krenn C R, Cohen M L and Morris J W Jr. 1999 *Phys. Rev. Lett.* **82** 2713
[37] Zhang Y, Sun H and Chen C F 2006 *Phys. Rev. B* **73** 144115
[38] Zhang R F, Veprek S and Argon A S 2008 *Phys. Rev. B* **77** 172103
[39] Chen X Q, Fu C L and Podloucky R 2008 *Phys. Rev. B* **77** 064103
[40] Guo W F, Wang L S, Li Z P, Xia M R and Gao F M 2015 *Chin. Phys. Lett.* **32** 096201
[41] Gao F M, He J L, Wu E D, Liu S M, Yu D L, Li D C, Zhang S Y and Tian Y J 2003 *Phys. Rev. Lett.* **91** 015502
[42] Gao F M, Xu R and Liu K 2005 *Phys. Rev. B* **71** 052103
[43] Gao F M 2006 *Phys. Rev. B* **73** 132104
[44] Gutiérrez G, Menéndez-Proupin E and Singh A K 2006 *J. Appl. Phys.* **99** 103504
[45] Wu Z J, Zhao E J, Xiang H P, Hao X F, Liu X J and Meng J 2007 *Phys. Rev. B* **76** 054115
[46] Pugh S F 1954 *Philos. Mag. A* **45** 823
[47] Yoo C S, Kim M, Lim J, Ryu Y J and Batyrev I G 2018 *J. Phys. Chem. C* **122** 13054
[48] Li Z P, Gao F M and Xu Z M 2012 *Comput. Mater. Sci.* **62** 55
[49] Li Z P, Gao F M and Xu Z M 2012 *Phys. Rev. B* **85** 144115
[50] Pan Z C, Sun H and Chen C F 2007 *Phys. Rev. Lett.* **98** 135505
[51] Li Z P and Gao F M 2012 *Phys. Chem. Chem. Phys.* **14** 869
[52] Chen X Q, Niu H, Li D and Li Y 2011 *Intermetallics* **19** 1275
[53] Chen X Q, Niu H, Franchini C, Li D Z and Li Y Y 2011 *Phys. Rev. B* **84** 121405
[54] Siethoff H 2000 *J. Appl. Phys.* **87** 3301
[55] Phillips J C 1970 *Rev. Mod. Phys.* **42** 317